A Repetition Scheme for MBSFN Based Mission-Critical Communications

Alaa Daher[1,2], M. Shabbir Ali[3], Marceau Coupechoux[1], Philippe Godlewski[1], Pierre Ngouat[4] and Pierre Minot[2]
[1]LTCI, Telecom ParisTech, University Paris-Saclay, France
{alaa.daher, marceau.coupechoux, philippe.godlewski}@telecom-paristech.fr
[2]ETELM, Les Ulis, France; {alaa.daher,pierre.minot}@etelm.fr
[3]Orange Labs, Châtillon, France; mdshabbirali88@gmail.com
[4]PNG-Technologies, Torcy, France; pierre.ngouat@png-technologies.com

***Abstract*—Mission-critical communications conveyed over Professional Mobile Radio (PMR) are characterized by a high level of reliability, an improved coverage and group call communications. Hybrid Automatic Repeat on re-Quest (HARQ) schemes are commonly used to provide a reliable communication over multipath noisy wireless channels. They, however, generate an excessive control signaling overhead on the uplink when downlink multicast is considered and groups include many members. In this paper, we propose a simple repetition scheme without request as an alternative to HARQ for group communications. When transport blocks are retransmitted several times, a tradeoff arises between coverage and capacity on the one hand, coverage and delay on the other hand. To evaluate the performance of our scheme, we use a link layer abstraction based on the Mean Instantaneous Capacity (MIC) together with BLER vs. SNR curves in AWGN. We carefully design our repetition scheme by considering the channel characteristics and the delay constraint imposed by video codecs. We show that up to 11 dB gain in SNR is achieved when compared to a scheme without repetition. System level simulations show that cell radius can be multiplied by three in a Multicast/Broadcast Single Frequency Network (MBSFN).**

I. Introduction

Multicast/Broadcast Single Frequency Network (MBSFN) and Single-Cell Point-To-Multipoint (SC-PTM) are two point-to-multipoint technologies envisioned for Professional Mobile Radio (PMR), which convey business- and mission-critical communications [1]. Mission-critical networks are characterized by specific requirements such as reliability, coverage and the possibility to have group calls. Contrary to classical mobile networks, capacity is not the main issue in practical deployments[1]. In this paper, we thus focus on coverage improvement in presence of group calls by proposing a repetition scheme based on Chase Combining (CC) and Maximum Ratio Combining (MRC).

Hybrid Automatic Repeat on re-Quest (HARQ) is a classical technique to improve communication reliability. For a given BLock Error Rate (BLER) target, the required Signal-to-Interference-plus-Noise Ratio (SINR) is lowered as the number of retransmissions increases. The gain achieved in terms of SINR can then be translated in terms of cell coverage. In [2], the authors show that HARQ with full Incremental Redundancy (IR) offers the best throughput performance for high modulation schemes but at the cost of higher memory requirement. On the contrary, HARQ with CC is favored, when lower modulation schemes are assumed and memory is a limiting factor. As MBSFN uses robust Modulation and Coding Schemes (MCSs), CC is a natural choice. In [3], Kumagai et al. presented a maximal ratio combining Automatic Repeat on re-Quest (ARQ) scheme for Orthogonal Frequency-Division Multiplexing (OFDM), in which the frequency is changed at every retransmission in order to benefit from frequency diversity. Moreover, several studies have shown gains in both average system capacity and cell-edge data rates, when introducing the frequency diversity to the packet scheduler [4], [5].

HARQ suffers however from multiple drawbacks when group calls are considered. As the transmission is multicast, retransmissions should be performed according to the multiple feedbacks from the User Equipments (UEs) in the group. As the number of group members increases, the control signaling overhead on the feedback channel may drastically increase. Also MBSFN standards have not adopted so far the possibility of a feedback channel on the uplink.

Hence, in this paper, we propose an alternative approach which relies on CC repetitions without any feedback. This technique is widely used in Internet of Things (IoT) standards Sigfox, LoRa and NB-IoT for simplicity reasons and sometimes because of the absence of feedback [6]. Here, for PMR networks, we design the time and frequency shifts to be adopted for every repetition based on the channel characteristics and video codec constraints. The number of repetitions and their time-frequency distance is the result of a tradeoff between coverage and capacity on the one hand, and between coverage and delay on the other hand. We show by link and system level simulations that the proposed scheme provides a substantial gain in terms of SINR, and hence is an attractive option to enhance the network coverage for delay sensitive reliable group communications.

The rest of the paper is organized as follows: in Section II, we introduce the system models used in our evaluation. Next, we present the abstractions considered at link level to cope the transmission chain complexity in Section III. In Section IV, we describe the proposed repetition scheme. Section V presents

[1]As experienced by ETELM, a PMR manufacturer.

and discusses the simulation results. Finally, conclusions are summarized in Section VI.

II. System Models

In order to evaluate our proposed scheme, we rely on both link level and system level approaches.

A. Link Level Model

We consider an OFDM downlink channel. The received signal on the n-th subcarrier during the i-th OFDM symbol is given by:

$$r_n[i] = \sqrt{p_n}\Omega_n[i]s_n[i] + w_n[i] \quad (1)$$

where $n = 1, ..., N_{sc}$ and $i = 1, ..., N_{sym}$, N_{sc} is the number of subcarriers in a Resource Block (RB), N_{sym} the number of symbols in a subcarrier, p_n the power allocated to the n-th subcarrier, $\Omega_n[i]$ the complex channel gain of samples received at the n-th subcarrier during the i-th OFDM symbol, $s_n[i]$ is the symbol transmitted over the n-th subcarrier of the i-th symbol, and $w_n[i]$ is the noise modeled as zero-mean Gaussian random variable with variance σ_w^2.

The Signal-to-Noise Ratio (SNR) experienced at the l-th transmission on the n-th subcarrier during the i-th symbol ($\dot{\gamma}_n[i]$) is given by:

$$\dot{\gamma}_{n,l}[i] = \frac{|\Omega_n[i]|^2 p_n}{\sigma_w^2} \quad (2)$$

Furthermore, we assume that MRC is performed at the receiver, so that after L transmissions, the SNR experienced at the receiver, using CC, is given by:

$$\gamma_n[i] = \sum_{l=1}^{L} \dot{\gamma}_{n,l}[i] \quad (3)$$

where $\dot{\gamma}_{n,l}[i]$ is the SNR experienced at the l-th transmission over the n-th subcarrier during the i-th OFDM symbol.

B. Rayleigh Fading Simulation Model

In order to simulate the Rayleigh channel, we use the function `rayleighchan` from Matlab. This function implements the methodology described [7] for discrete multipath. In a nutshell, a discrete multipath channel model is used, in which the input $\{s_i\}$ is supposed to be band limited and the output can be written as:

$$y_i = \sum_{n=-N}^{N} s_{i-n} g_n, \quad (4)$$

where

$$g_n = \sum_{k=1}^{K} \check{\Omega}_k \operatorname{sinc}\left[\frac{\tau_k}{T} - n\right] \quad (5)$$

is the tap weight, $\check{\Omega}_k$ and τ_k are the path-gain and the delay of the k-th path respectively, and T is the sampling period.

Now path-gains $\check{\Omega}_k$ are obtained using a Sum-Of-Sinusoids (SOS) approach, like for the Jakes model [8]. The SOS method implemented in Matlab [9] is the Pätzold model [10], it overcomes some of the limitations of Jakes model.

In this model, the received field over a path at the receiver is made of the superposition of several sinusoids, each with an amplitude, a phase and an angle of arrival. More specifically, the received field from the k-th path ($k = 1, 2, ..., K$) is expressed as:

$$\begin{aligned} \mu_k(t) &= \mu_{I,k}(t) + j\mu_{Q,k}(t) \\ \mu_{I,k}(t) &= \sqrt{\frac{2}{M_k}} \sum_{m=1}^{M_k} \cos(2\pi f_{I,m,k} t + \phi_{I,m,k}) \quad (6) \\ \mu_{Q,k}(t) &= \sqrt{\frac{2}{M_k}} \sum_{m=1}^{M_k} \cos(2\pi f_{Q,m,k} t + \phi_{Q,m,k}) \end{aligned}$$

where M_k specifies the number of sinusoids used to model the k-th path; $\phi_{I,m,k}$ and $\phi_{Q,m,k}$ refer to the phase of the m-th components of $\mu_{I,k}(t)$ and $\mu_{Q,k}(t)$ respectively and are independently and identically distributed random variables having a uniform distribution over $[0; 2\pi]$; $f_{I,m,k}$ and $f_{Q,m,k}$ are the discrete Doppler frequencies of the in-phase and quadrature components respectively, calculated for each component within a single path, and are given by:

$$\begin{aligned} f_{I,m,k} &= f_D \cos\left[\frac{\pi}{2M_k}(m - \frac{1}{2}) + \frac{\pi}{4M_k} \cdot \frac{k}{K+2}\right] \quad (7) \\ f_{Q,m,k} &= f_D \cos\left[\frac{\pi}{2M_k}(m - \frac{1}{2}) - \frac{\pi}{4M_k} \cdot \frac{k}{K+2}\right], \end{aligned}$$

where $f_D = \frac{v f_c}{c}$ is the maximum Doppler shift, f_c is the carrier frequency, v is the terminal speed, and c is the speed of light. From this process, the path-gain is obtained by scaling the result with the average path-gain:

$$\check{\Omega}_k = \sqrt{E(|\check{\Omega}_k|^2)}\mu_k. \quad (8)$$

C. System Level Model

For system level simulations, we consider the downlink of a cellular network with omnidirectional evolved Nodes-B (eNBs) implementing either MBSFN or SC-PTM transmissions and we adopt the model in [1]. The SINR with SC-PTM is computed as for a unicast transmission. With MBSFN all stations from the MBSFN area emit useful signal, whereas all stations outside this area contribute to interference. The inter-symbol interference caused by delays exceeding the cyclic prefix is taken into account. Channel model includes distance dependent path-loss and lognormal shadowing. See [1] for more details.

III. Link Level Abstraction

At link level, we adopt a simplified methodology to allow us obtaining very quick results for various scenarios compared to the simulation of a complete transmitter-receiver chain.

A. Overall Architecture

The overall architecture is shown in Fig. 1. On the left hand side, we use an existing link level simulator, e.g., the Matlab LTE Toolbox [11] or the Vienna LTE Simulator [12]. We generate a BLER vs. SNR curve in Additive White Gaussian

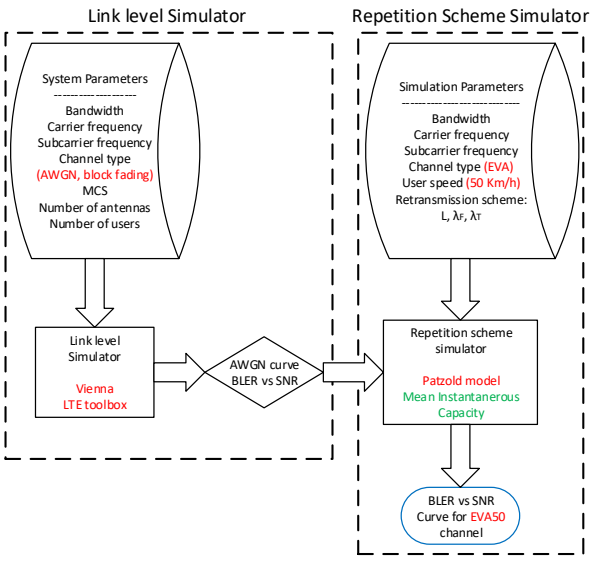

Fig. 1: Link Level Methodology.

Noise (AWGN) for a given set of input parameters including e.g. the Modulation and Coding Scheme (MCS), number of antennas, bandwidth, etc. This curve is an input of our simulator (right hand side of the figure) together with the Rayleigh fading channel to be simulated and the repetition scheme we aim to evaluate.

The repetition scheme simulator generates a fading channel according to the method described in Section II-B, computes the effective SNR and evaluate the BLER for every RB thanks to the BLER vs. SNR curve in AWGN. This approach allows to quickly test various repetition schemes on various channels and speeds. One point on the BLER vs. SNR curve is obtained in few minutes compared to possibly several hours with a complete link level simulator (on a Mac Book Pro 2.6GHz Intel Core i5).

B. Effective SNR

In order to evaluate the radio link quality over a RB j of N_{sc} subcarriers and N_{sym} OFDM symbols, we adopt the Mean Instantaneous Capacity (MIC) approach. Other similar link layer abstractions exist, such as Exponential Effective SNR Mapping (EESM) (see e.g. [13]), but MIC has the advantage to be simple, to have an information theoretical interpretation and still provide good results [14]. The first step in this method is to determine the instantaneous capacity of the n-th subcarrier at the i-th OFDM symbol over the j-th RB using Shannon's formula:

$$C_n^{(j)}[i] = \log_2(1 + \gamma_n^{(j)}[i]), \tag{9}$$

where $\gamma_n^{(j)}[i]$ is the SNR experienced on subcarrier n, at symbol i and RB j. The MIC is then computed by averaging over the $N_{sc} \times N_{sym}$ Resource Elements:

$$MIC_j = \frac{1}{N_{sc} \times N_{sym}} \sum_{n=1}^{N_{sc}} \sum_{i=1}^{N_{sym}} C_n^{(j)}[i]. \tag{10}$$

The effective SNR is then given in terms of MIC value by [14]:

$$\gamma_{eff}^{(j)} = 2^{MIC_j} - 1. \tag{11}$$

C. BLER Evaluation

The effective SNR is now mapped to BLER versus SNR curves in AWGN to estimate the BLER of the transmitted block, i.e., the probability that this block is erroneous. More specifically, a $BLER_j$ is associated to RB j as follows:

$$BLER_j = BLER_{AWGN}(\gamma_{eff}^{(j)}) \tag{12}$$

where $BLER_{AWGN}$ represents the BLER vs. SNR curve for the AWGN channel, obtained by link level simulator.

IV. Repetition Scheme

In this section, we present our repetition scheme justified by design principles.

A. Design Principles

The way repetitions are performed depends on the channel characteristics and video constraints.

1) Coherence Bandwidth: In a scattered environment, the received signals arrive along different paths with different power attenuation and delays. The Root Mean Square (RMS) delay spread is a measure of the time dispersion of the channel and can be obtained from the power delay profile as follows [7]:

$$\delta_t = \sqrt{\frac{\sum_{k=1}^{K} P_k(\tau_k - \bar{\tau})^2}{\sum_{k=1}^{K} P_k}}, \tag{13}$$

where P_k is the power attenuation in path k, τ_k is the path delay, and $\bar{\tau}$ is the mean excess delay given by:

$$\bar{\tau} = \frac{\sum_{k=1}^{K} P_k \tau_k}{\sum_{k=1}^{K} P_k}. \tag{14}$$

From the RMS delay spread, we deduce the coherence bandwidth (B_c). It is a statistical measure of the range of frequencies over which the channel can be considered flat, i.e., a channel which passes all spectral components with approximately equal gain and linear phase. If the coherence bandwidth is defined as the bandwidth over which the frequency correlation function is above 0.5, then the coherence bandwidth is approximately [7], [15]:

$$B_c \approx \frac{1}{5\delta_t} \tag{15}$$

In order to achieve a maximum diversity, it is desirable that repetitions occur in frequency at a distance greater than the coherence bandwidth. PMR mission-critical networks are expected to be operated in 5 MHz bandwidth, which gives an upper limit for frequency separation between two repetitions. In Tab. I, we provide some examples of coherence bandwidths for some typical multipath fading environments, deduced from the corresponding power delay profile [16].

Multi-path propagation channel	Coherence Bandwidth (B_c)
Extended Pedestrian A (EPA)	4.6 MHz
Extended Vehicular A (EVA)	540 kHz
Extended Typical Urban (ETU)	200 kHz

TABLE I: Coherence Bandwidth of typical multi-path fading channels.

2) Coherence Time: The time varying nature of the channel in a small-scale region can be described by the Doppler spread and coherence time. The coherence time is a statistical measure of the time duration over which the channel impulse response is invariant, and quantifies the similarity of the channel response at different times. Coherence time (T_c) and Doppler spread (f_D) are inversely proportional to each other:

$$T_c \approx \frac{1}{f_D} \tag{16}$$

It is desirable to perform repetitions beyond the coherence time of the channel. However, as the number of repetitions increases, delay increases as well. In video traffic, there is an upper limit beyond which this delay becomes unacceptable. PMR networks operate at 700 MHz, thus, we can deduce the coherence time for typical User Equipment (UE) speeds, see Tab. II.

UE speed	3 km/h	50 km/h	120 km/h
Coherence Time (T_c)	514 ms	31 ms	1.3 ms

TABLE II: Coherence time of typical PMR UE speed.

3) Video Quality Constraints: Group calls for mission-critical communications are subject to video quality constraints. Several approaches have been proposed to predict the video Quality of Experience (QoE) through objective video quality metrics with the goal of not relying on human evaluations. Peak Signal to Noise Ratio (PSNR) of the decoder luminance reconstruction [17] and the Structural SIMilarity (SSIM) [18] are such examples.

However, to keep things simple, we retain in this paper only the constraints on the BLER and the average delay between two frames. A more accurate evaluation of the video quality is left for further work. In [19], Solera et al. use an emulator to evaluate video services over Long Term Evolution (LTE) networks and assume a fixed target BLER of 10%. Moreover, in [20], the PSNR is evaluated in terms of BLER, and the system performance is studied for a target BLER of 10%. Based on these references, we adopt this constraint for the BLER.

A typical video codec over wireless is H264 Level 1.2 with 320x240 resolution, maximum transmission rate of 384 kbps, and frame rate of 20 fps. In order to receive all retransmitted copies of a given frame before the transmission of the next one, the maximum transmission time of each frame shouldn't thus exceed 50 ms. The maximum intra-frame period allowed is then $50/(L-1)$ ms when L transmissions are performed. This gives us an upper bound on the delay between two repetitions, e.g., 16 ms when $L = 4$.

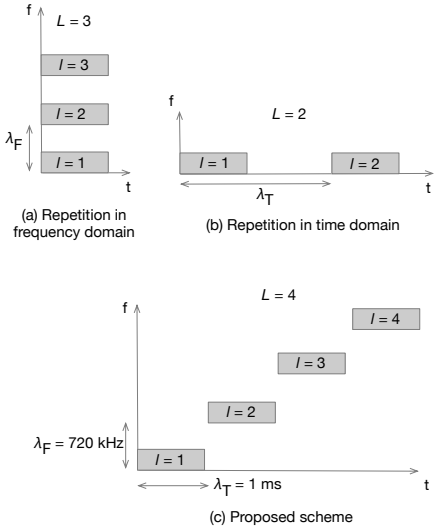

Fig. 2: Repetition Schemes.

B. Proposed Scheme

A repetition scheme is characterized by the triplet $(L, \lambda_F, \lambda_T)$, where L is the number of repetitions, λ_T is the time delay and λ_F the frequency hopping step between two consecutive repetitions. Fig. 2 (a) and (b) show two such schemes where only the frequency or the time degrees of freedom are exploited respectively.

Owing to the design principles described above and the simulation results, the proposed scheme adopt $L = 4$, $\lambda_F = 720$ kHz (4 RBs) and $\lambda_T = 1$ ms (1 Transmission Time Interval (TTI)), see Fig. 2 (c). As shown in the next section, $L = 4$ offers a good tradeoff between coverage and capacity. The choice of λ_F (1 RB above the coherence bandwidth) provides significant diversity gains with the channel EVA50, i.e., for mission-critical communications deployed in a urban environment. It also allows an easy multiplexing of the group calls within the 25 RBs by cyclically shifting in frequency the next transmission while never violating the 4 RBs distance. The choice of λ_T ensures that the delay constraint is met. It doesn't provide much more gain compared to $\lambda_T = 0$ but allows the application of the scheme on the uplink as well. Indeed, a user terminal can then concentrate its transmit power on every transmissions, while with $\lambda_T = 0$ it would have shared its power between transmitted RBs. Higher uplink coverage is thus expected with the proposed delay.

V. Simulation Results

In this section, we present the evaluation results of the proposed repetition scheme.

A. Simulation Parameters

Simulation parameters are shown in Tab. III. We consider an EVA multipath channel for a group of users moving at 50 km/h. We use typical parameters for PMR networks, e.g., a carrier frequency of 700 MHz, a bandwidth of 5 MHz, and for MBSFN, e.g., a fixed robust MCS and extended cyclic prefix.

Parameter	Assumption
Carrier frequency (f_c)	700 MHz
Duplexing	Frequency Division Duplex (FDD)
Bandwidth (B)	5 MHz
Sampling frequency	7.68 MHz
Nb. of subcarriers per RB (N_{sc})	12 subcarriers
Nb. of OFDM symbols (N_{sym})	12 symbols/TTI
Number of simulated TTI	10000 TTI
Modulation and coding scheme	MCS 2 [21, Table 7.1.7.1-1A]
Fast Fourier Transform size	512
Subcarrier bandwidth	15 KHz

TABLE III: Simulation parameters.

B. Validation of the Link Level Abstraction

Fig. 3 shows the comparison between the link level abstraction and link level simulations. Link level simulations have been obtained with the Matlab LTE toolbox and with the LTE Vienna simulator assuming EVA50 channel. Link level abstraction curves have been obtained using the methodology presented in Section III that relies on AWGN curves and MIC. We see that curves deviates for BLERs lower than 10^{-2} but match well at the target BLER of 10^{-1} we are studying.

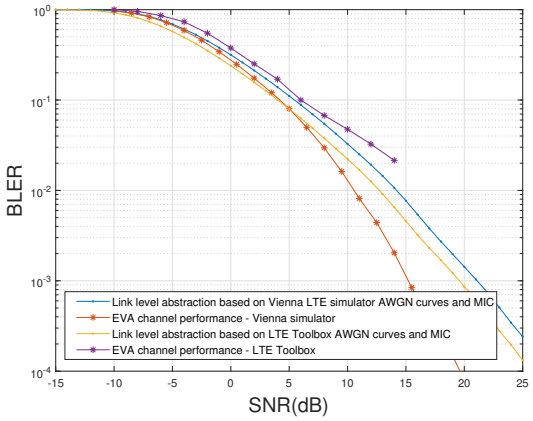

Fig. 3: Comparison between link level abstraction and link level simulations using Matlab LTE Toolbox or Vienna LTE simulator.

C. Repetition Scheme Results

In Fig. 4, we show the performance of different repetition schemes characterized by different number of repetitions (L), time delays (λ_T) and frequency hopping steps (λ_F). In Fig. 4a, when $\lambda_F = 0$ and $\lambda_T = 1$ ms, a constant gain is observed for every L when the SNR increases. Gains of 3, 5 and 6 dB are observed for $L = 2$, 3, and 4 respectively over $L = 1$. This is due to the increase of received power at the receiver.

When either λ_F or λ_T are increased, a diversity gain is also observed, especially when these parameters are larger than the coherence bandwidth and time, respectively. As expected, best performances are achieved when $\lambda_F = 720$ kHz and $\lambda_T = 32$ ms. By comparing the left and right sides of Fig. 4, we however see that frequency diversity has more impact than time diversity with the chosen values.

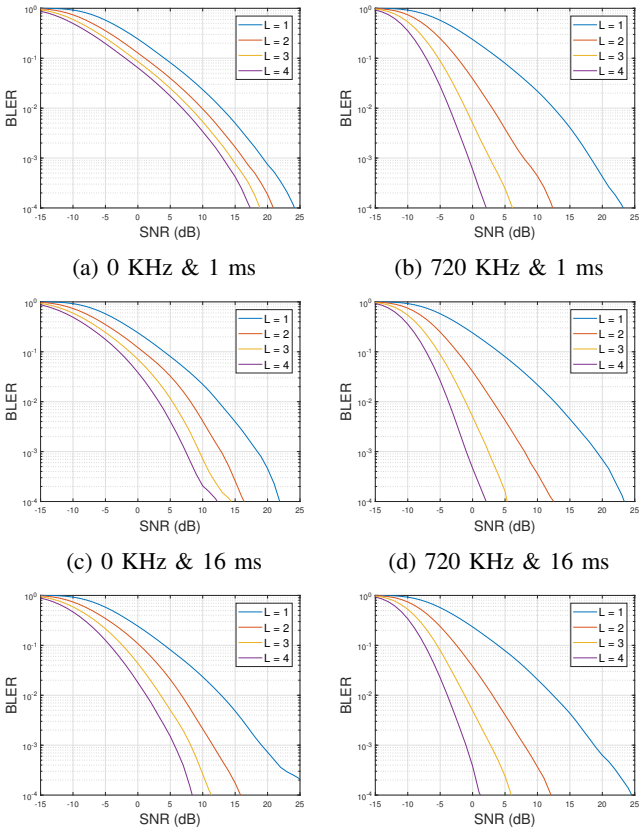

(a) 0 KHz & 1 ms (b) 720 KHz & 1 ms

(c) 0 KHz & 16 ms (d) 720 KHz & 16 ms

(e) 0 KHz & 32 ms (f) 720 KHz & 32 ms

Fig. 4: BLER vs. SNR for various frequency hopping steps and time delays and for $L = 1$, 2, 3, and 4 repetitions.

This is confirmed by Fig. 5, which shows the SNR threshold required to reach the BLER target of 10^{-1} as a function of the number of repetitions L for different repetition schemes. It is clear that increasing the frequency distance between repetitions is much more effective than increasing the delay. Moreover, when $\lambda_F = 720$ kHz is chosen, increasing the delay has a negligible impact. The reason lies in the delay constraint that prevents us to fully benefit from time diversity. Considering higher values of L would lead to small SNR gains at the cost of a loss of capacity. With the proposed scheme ($L = 4$, $\lambda_F = 720$ kHz and $\lambda_T = 1$ ms), we have a 11 dB gain compared to $L = 1$ (today's scheme in MBSFN), 5 dB gain over consecutive repetitions ($L = 4$, $\lambda_F = 0$ and $\lambda_T = 1$ ms) and 3 dB gain over repetitions solely in time ($L = 4$, $\lambda_F = 0$ and $\lambda_T = 16$ ms, the maximum delay allowed by the video codec).

D. Cell Radius Gain

In order to evaluate the cell coverage gains, we adopt the model used in [1] to estimate the achievable cell range in a urban environment for a SFN120 configuration (group members are in 1 cell, there are 2 rings of MBSFN area and there is no reserved cell), based on SNR thresholds presented in Fig. 5, for an outage probability of 2%. The results are summarized in Fig. 6. With the proposed scheme, cell radius

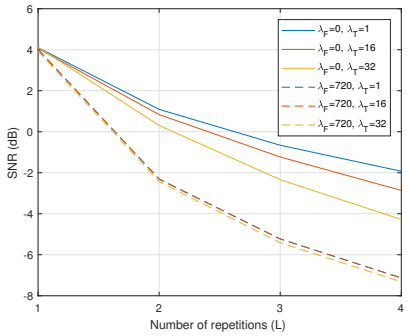

Fig. 5: SNR thresholds for different repetition schemes at target $BLER = 10^{-1}$ (λ_F in kHz and λ_T in ms).

increases from 600 m to 2000 m compared to a network without repetitions. Cell radius is also improved by 50% compared to successive repetitions ($L = 4$, $\lambda_F = 0$ and $\lambda_T = 1$ ms). Again, there is no need to implement high delay shift when $\lambda_F = 720$ kHz.

SC-PTM is an alternative to MBSFN introduced in Release R13 that activates only cells to which group users are attached. This is a solution to increase capacity at the cost of coverage. Our repetition scheme can be used with SC-PTM as well. In Fig. 6, we show that SC-PTM in conjunction with our scheme can provide higher cell range than traditional MBSFN without repetition.

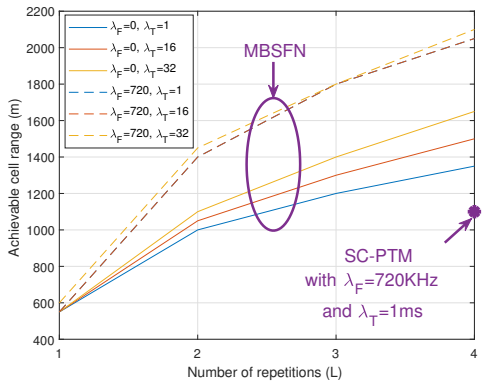

Fig. 6: Achievable cell range in MBSFN and SC-PTM urban networks for a target $BLER = 10^{-1}$ and outage probability of 2% (λ_F in kHz and λ_T in ms).

VI. Conclusion

In this paper, a repetition scheme adopted for PMR networks using MBSFN and SC-PTM to convey group communications is proposed and evaluated in terms of SNR and cell coverage gains. The proposed scheme takes into account the coherence bandwidth and the coherence time of the multipath fading channel together with service delay constraints. The comparison between different schemes show that frequency shifts between repetitions significantly improves the network performance, while time diversity increases transmission delay without bringing important gains. Simulation results show that an SNR gain of 11 dB can be achieved over classical MBSFN transmissions without repetitions. This translates in a cell range multiplied by three in a urban environment. The proposed scheme could be adopted for next MBSFN and SC-PTM standard releases as an attractive option to increase cell coverage for mission-critical communications.

References

[1] A. Daher, M. Coupechoux, P. Godlewski, P. Ngouat, and P. Minot, "SC-PTM or MBSFN for Mission Critical Communications?," in *2017 IEEE 85th Vehicular Technology Conference (VTC Spring)*, vol. 2017-June, pp. 1–6, IEEE, 6 2017.

[2] K. C. Beh, A. Doufexi, and S. Armour, "Performance Evaluation of Hybrid ARQ Schemes of 3GPP LTE OFDMA System," in *2007 IEEE 18th International Symposium on Personal, Indoor and Mobile Radio Communications*, pp. 1–5, IEEE, 2007.

[3] T. Kumagai, M. Mizoguchi, T. Onizawa, H. Takanashi, and M. Morikura, "A maximal ratio combining frequency diversity ARQ scheme for OFDM signals," in *1998 IEEE 9th International Symposium on Personal, Indoor and Mobile Radio Communications*, pp. 528–532, IEEE, 1999.

[4] A. Pokhariyal, T. Kolding, and P. Mogensen, "Performance of Downlink Frequency Domain Packet Scheduling for the UTRAN Long Term Evolution," in *2006 IEEE 17th International Symposium on Personal, Indoor and Mobile Radio Communications*, pp. 1–5, IEEE, 2006.

[5] C. Wengerter, J. Ohlhorst, and A. Golitschek Edler von Elbwart, "Fairness and Throughput Analysis for Generalized Proportional Fair Frequency Scheduling in OFDMA," *2005 IEEE 61st Vehicular Technology Conference*, vol. 3, no. 2, pp. 1903–1907, 2005.

[6] H. Wang and A. O. Fapojuwo, "A Survey of Enabling Technologies of Low Power and Long Range Machine-to-Machine Communications," *IEEE Communications Surveys & Tutorials*, vol. 19, no. 4, pp. 2621–2639, 2017.

[7] M. Jeruchim, P. Balaban, and K. Shanmugan, *Simulation of communication systems: modeling, methodology, and techniques*. Springer Science & Business Media, 2000.

[8] W. Jakes, *Microwave Mobile Communications*. Wiley-IEEE Press, 1974.

[9] C.-D. Iskander, "A MATLAB-based Object-Oriented Approach to Multipath Fading Channel Simulation," 2016. Available on mathworks.com.

[10] M. Patzold and B. Hogstad, "Two New Methods for the Generation of Multiple Uncorrelated Rayleigh Fading Waveforms," *2006 IEEE 63rd Vehicular Technology Conference*, vol. 6, no. 6, pp. 3122–3131, 2006.

[11] "Simulate, analyze, and test the physical layer of LTE and LTE-Advanced wireless communications systems," 2017. The MathWorks, Natick, MA, USA. Available on mathworks.com.

[12] C. Mehlfuhrer, M. Wrulich, J. C. Ikuno, D. Bosanska, and M. Rupp, "Simulating the long term evolution physical layer," *17th European Signal Processing Conference (EUSIPCO 2009), Glasgow, Scotland*, vol. 27, no. Eusipco, p. 124, 2009.

[13] X. He, K. Niu, Z. He, and J. Lin, "Link layer abstraction in MIMO-OFDM system," *2007 International Workshop on Cross Layer Design, IWCLD 2007*, pp. 41–44, 2007.

[14] K. Ramadas and R. Jain, "WiMAX system evaluation methodology," in *Wimax Forum, Jan*, 2007.

[15] J. G. Proakis and M. Salehi, *Digital Communications*. McGraw-Hill Higher Education, 2001.

[16] 3GPP, "Base Station (BS) radio transmission and reception," TS 36.104, 3rd Generation Partnership Project (3GPP), Sept. 2017.

[17] Q. Huynh-Thu and M. Ghanbari, "Scope of validity of PSNR in image/video quality assessment," *Electronics Letters*, vol. 44, no. 13, p. 800, 2008.

[18] Z. Wang, A. Bovik, H. Sheikh, and E. Simoncelli, "Image Quality Assessment: From Error Visibility to Structural Similarity," *IEEE Transactions on Image Processing*, vol. 13, pp. 600–612, 4 2004.

[19] M. Solera, M. Toril, I. Palomo, G. Gomez, and J. Poncela, "A Testbed for Evaluating Video Streaming Services in LTE," *Wireless Personal Communications*, vol. 98, no. 3, pp. 1–21, 2017.

[20] R. Zhang, S. L. Regunathan, and K. Rose, "Video coding with optimal inter/intra-mode switching for packet loss resilience," *IEEE Journal on Selected Areas in Communications*, vol. 18, no. 6, pp. 966–976, 2000.

[21] 3GPP, "Physical layer procedures," TS 36.213, 3rd Generation Partnership Project (3GPP), Jan. 2016.